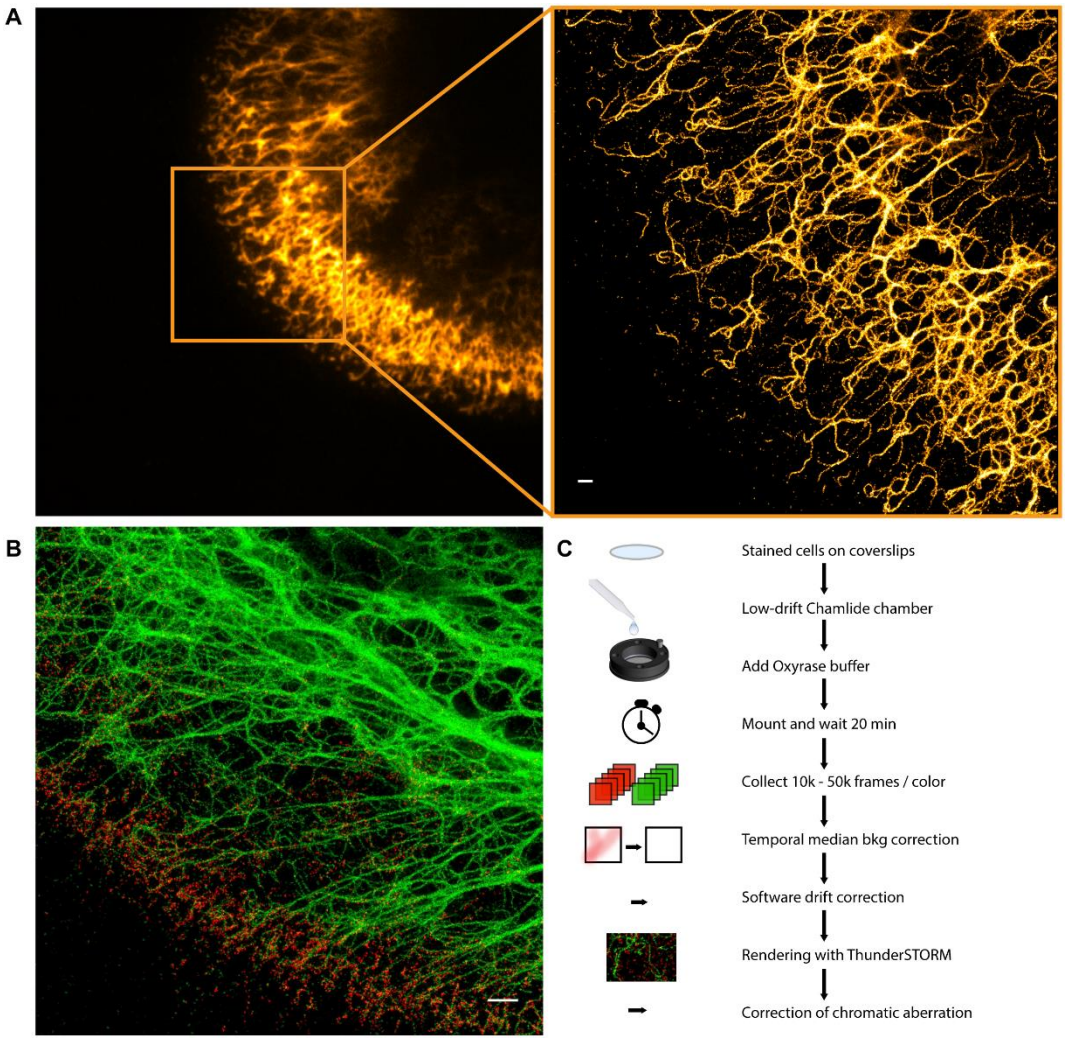

Figure S1. Imaging the fine keratin filament network in the periphery of the cell.
(A) Keratin filaments observed by TIRF (left) and SR microscopy (right). The SR image shows individual filaments running parallel to the basal membrane. The filaments in the outer rim of the cell are thinner in diameter. Scale bar: 500 nm. (B) Optimized two-color SR image of keratin and plectin. Scale bar: 500 nm. (C) Schematic overview of the various optimized acquisition and correction steps to obtain the highly-corrected two- and three-color GSD images in this paper.

Coverslips with stained cells were mounted in a Chamlide CMB magnetic chamber (Live Cell Instrument, Seoul, South Korea). Of several commercial dishes and holders, the Chamlide holders were found to have minimal drift, as detected by analyzing long time-lapse image series taken from coverslips with sparse sub-resolution fluorescent beads (Invitrogen). Popular imaging buffers for SR microscopy are typically optimal only for a single channel (fluorescent dye). Since physicochemical blinking mechanisms may vary widely between different dyes, the fluorophores in extra channels (second- and third colors) show suboptimal blinking kinetics and brightness, leading to significantly diminished image quality in these channels. We tested several alternative buffer formulations, aiming specifically to optimize blinking for two- and three-dye SR imaging and thereby obtain high quality multi-color images.

These tests resulted in a new oxygen scavenging buffer, termed OXEA (a mixture of mercaptoethylamine (50 mM), the oxygen scavenger system Oxyrase (OXYRASE Inc, Mansfield, Ohio, USA, 3%) and sodium-L-lactate (12%, w/w) in PBS). We found that this buffer supports fast and bright blinking of Alexa Fluor-647, AF-488 and AF-532 for two- and three-color imaging (full details to be published elsewhere). After addition of 500 µl of OXEA to the coverslips, cells were mounted on the microscope and the preparation was left to stabilize for 15-30 min to avoid initial drift before SR data were acquired. A total of 10.000 to 50.000 frames (10 ms) were collected for each channel. Blinking detection threshold was set at 70 photons/pixel (~500 photons/event). For 2-color imaging, the Alexa-647 channel was imaged first, followed by Alexa-488. These two dyes show essentially no leak-through. For 3-color SR imaging, we first imaged Alexa-647, followed by Alexa-488 (with 500/30 band-pass filter to prevent leak-through of Alexa-532). Thereafter, Alexa-488 had bleached enough to prevent leak through in the third channel, Alexa-532. For post-acquisition correction steps, data were transferred to an off-line workstation. First, we applied our temporal median background correction (Hoogendoorn et al., Scientific Reports 2014) to the raw data using home-built software (available on request). This correction proved especially powerful to improve the image quality in densely labeled structures. Following that, any residual X/Y drift was removed from the data using a home-built 'de-jittering' routine. For image rendering, the Image J plugin ThunderSTORM (Ovesny et al., Bioinformatics 2014) was used with final pixel size of 10 nm and, if many events were present, additional filtering to reject the least precise localizations. Alternatively, the built-in de-jittering algorithm of recent versions of ThunderSTORM was used. As a final step, chromatic aberrations (CA) were precisely corrected. CA (of up to 60 nm) was mapped throughout the focal plane by imaging 0.1 µm diameter Tetraspec microspheres (Invitrogen) embedded in a matrix. An affine transformation matrix was constructed from those data and affine correction of all images was carried out using a home-build ImageJ macro (available on request). CA was highly stable over several months of imaging. While elaborate, these improvements allowed us to routinely obtain very good quality two- and three-color images.

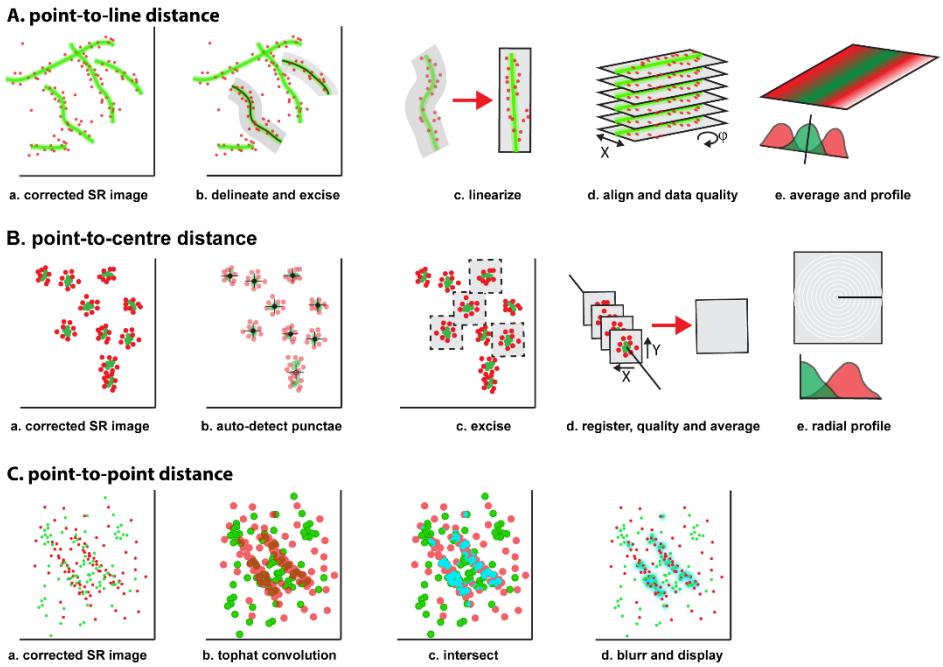

Figure S2. Calculation of molecular distance distributions and proximity mapping.
(A) Determining the distribution of distances between one label decorating a filament and an arbitrary second label. In SR images (a) containing filaments and additional label(s), the centers of individual un-branched filaments was delineated manually by drawing curved lines (b) of 500 nm width onto the keratin channel. We made sure that filaments were single-stranded and well-separated so as to avoid potential overlap with nearby filaments. Then each of the selected curved Regions Of Interest (ROI) surrounding a single filament was excised (b) and linearized (c) using the straightening (affine transformation) routine in ImageJ. This routine warps the image so as to linearize the curved lines as well as the image area surrounding it. Because radius of curvature is very large in relationship to the detected distances, this does not alter the average distances of individual points (β4, etc.) to the linearized filaments. The straightened filaments (ROIs) were precisely oriented vertically by image rotation, divided up in shorter line segments of ~1 μm long and centered laterally with sub-pixel resolution (d) by Gaussian fitting of the intensity profile of the filaments. This automated alignment procedure (macro available on request) corrects for slight inaccuracies in tracing, and it allows for data cleanup by discarding those sub-images in which the Gaussian fit does not fulfill constraints on filament width and goodness-of-fit. To calculate the distribution of distances between keratin and the second color channel (integrin β4, plectin, BP230 or BP180) the sub-images were summed and projected onto a line orthogonal to the filament direction (e). Validity of this analysis was verified by analyzing synthetic (in silico) data sets with our routines. These tests showed that the affine transformation and alignment routines did not affect average measured distances, while only a very slight (~ 1 nm) effect was observed on the width of the distribution. (B) To detect radial distances in the circular patterns of BP230 and BP180 (a), punctae of bright staining were detected by thresholding and size-exclusion based on the BP230 channel (b), and the surrounding regions of interest (200 x 200 nm) (c) were copied into an ROI image dataset. Excised ROIs were automatically aligned with sub-pixel precision based on the center of gravity of the BP230 signal (d), and the average image of all data was constructed for both channels (d, below). The intensity-distance distribution was then made by averaging the intensities in concentric circles with indicated radii to the center of BP230 (e). (C) To produce pixel maps that visualize molecular proximity (at a user-selected scale), the two color channels (a) are convolved with a normalized 2D circular top-hat kernel of size *R* (b), which evenly dilates individual bright pixels over a range *R* while keeping the integrated intensity unchanged. On the resulting images conventional colocalization was applied using thresholding according to Costes method (Costes et al., 2004), after which local proximity was computed as (SQRT (gray value$_{channel1}$ x gray value$_{channel\ 2}$)) (c). This procedure thus yields a proximity map that depicts vicinity of the two colors up to a scale *R*. This method can be extended to show proximity in a distance *r* (range 0<*r*<*R)* by subtracting two proximity maps produced with kernel sizes *R* and *r*. By overlaying the *proximity map* with the original multicolor Super-Resolution image (d), the places in the image where the two labels are in close vicinity are clearly marked visually. As control, no significant proximity was observed between β4 and an Ab against an unrelated membrane protein, MHC heavy chain. All data analysis was based on the nr of ROIs indicated in the text. ROIs were selected from 7-30 individual cells, and each experiment was carried out at least 5 times on separate days. Further information and software routines may be obtained by emailing k.jalink@nki.nl

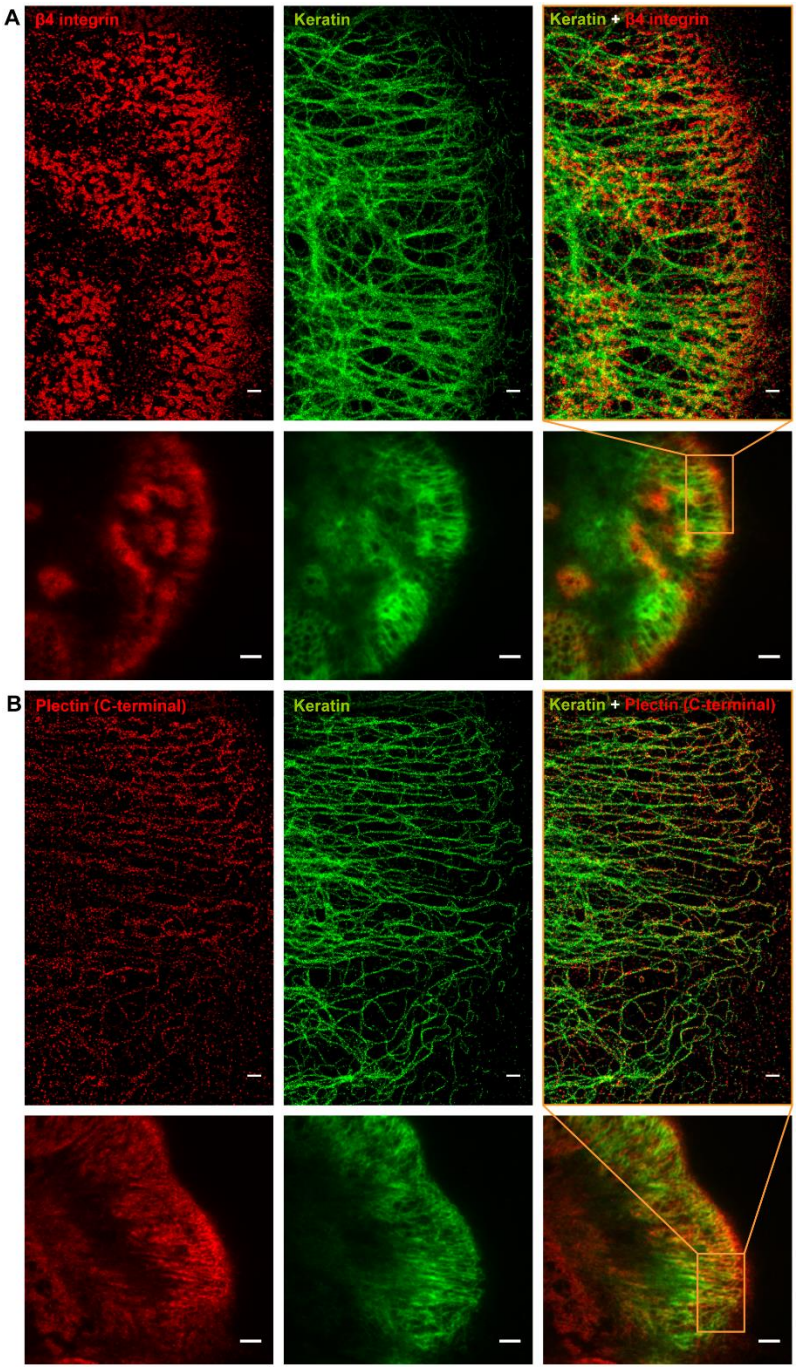

Figure S3. Comparison of the distribution of β4 and plectin with keratin-14 in PA-JEB/β4 keratinocytes. Representative high-resolution images of cells stained for keratin-14 and β4 integrin (A) or for keratin-14 and plectin (B; Ab against the C-terminus), together with the TIRF images to provide cellular context. Note that the pdf images allow zoom-in to 10 nm resolution. Scale bars are 500 nm (3 μm for TIRF images).

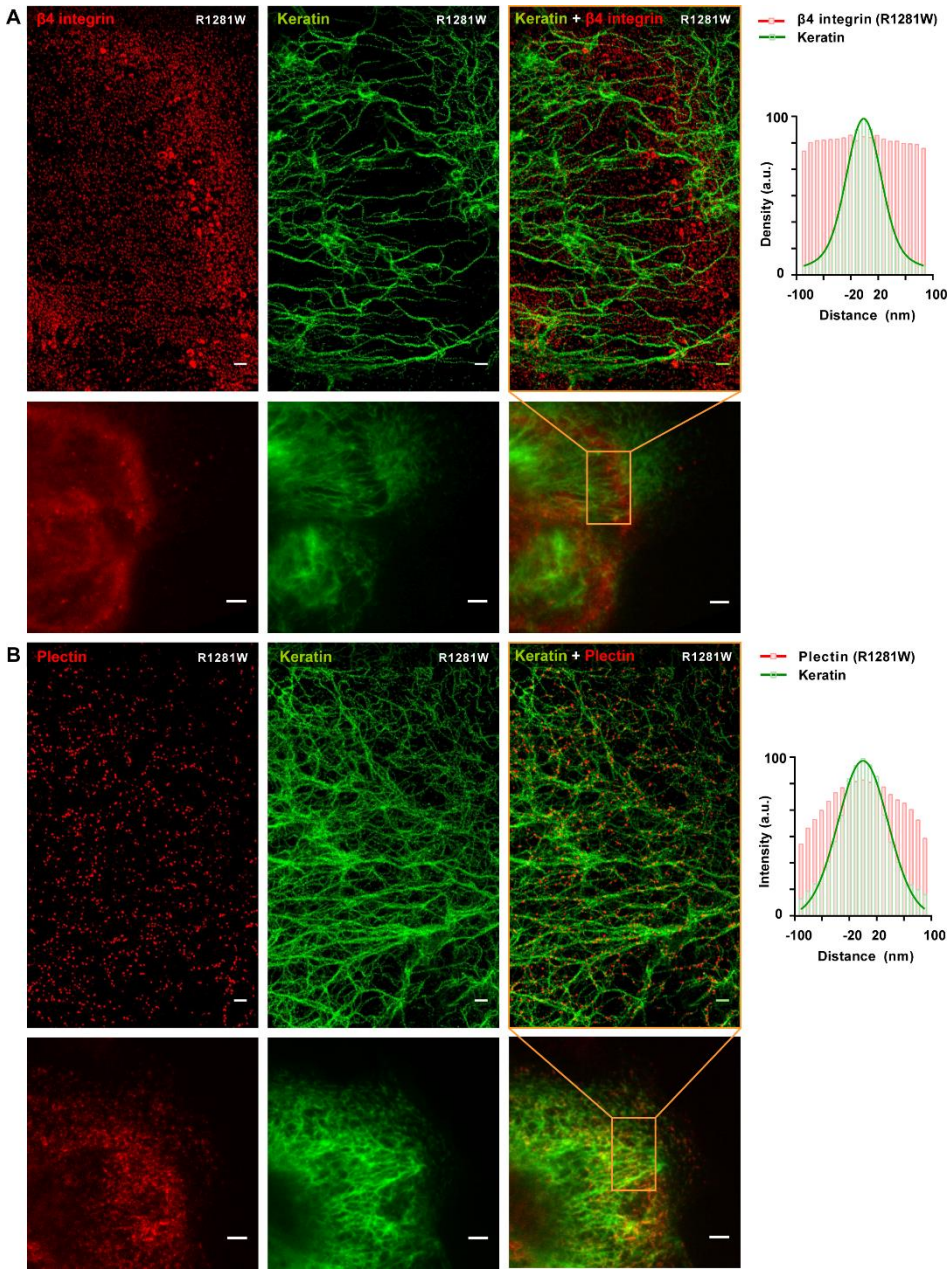

Figure S4. Comparison of the distribution of β4 and plectin with keratin-14 in PA-JEB keratinocytes expressing β4 ^{R1281W}.

(A) High-resolution and TIRF images of cells stained for keratin-14 and β4 integrin. The graph showing the distance distribution between plectin and keratin-14 is identical to that in Fig. 1B. It illustrates that there is no specific distribution of β4 along the keratin filaments in these cells. (B) High-resolution and TIRF images of keratin-14 and plectin (Ab against rod domain). The graphs show the distance distribution between plectin and keratin-14 in PA-JEB keratinocytes expressing mutant β4 ^{R1281W}. Because the β4 mutant cannot interact with plectin, plectin is no longer held in position along keratin filaments but is flexible. The consequent change in distribution from bi-modal (Fig. 2C; wt β4) to unimodal (β4 R1281W) supports the tent-and-peg model. Average results are shown from n=160 ROIs taken from n=8 cells. Scale bars are 500 nm (3 μm for TIRF images).

References:

Costes, S.V., Daelemans, D., Cho, E.H., Dobbin, Z., Pavlakis, G., and Lockett, S. (2004). Automatic and quantitative measurement of protein-protein colocalization in live cells. *Biophys J*. 86, 3993-4003.

Hoogendoorn, E., Crosby, K.C., Leyton-Puig, D., Breedijk, R.M., Jalink, K., Gadella, T.W., and Postma, M. (2014). The fidelity of stochastic single-molecule super-resolution reconstructions critically depends upon robust background estimation. *Sci. Rep*. 4, 3854.

Ovesný, M., Křížek, P., Borkovec, J., Svindrych, Z., and Hagen, G.M. (2014). ThunderSTORM: a comprehensive ImageJ plug-in for PALM and STORM data analysis and super-resolution imaging. *Bioinformatics* 30, 2389-2390.